

# Causal SHAP: Feature Attribution with Dependency Awareness through Causal Discovery

Woon Yee Ng\*, Li Rong Wang\*, Siyuan Liu\*, and Xiuyi Fan†\*

\*College of Computing and Data Science,

†Lee Kong Chian School of Medicine,

Nanyang Technological University, Singapore

**Abstract**—Explaining machine learning (ML) predictions has become crucial as ML models are increasingly deployed in high-stakes domains such as healthcare. While *SHapley Additive exPlanations* (SHAP) is widely used for model interpretability, it fails to differentiate between causality and correlation, often misattributing feature importance when features are highly correlated. We propose *Causal SHAP*, a novel framework that integrates causal relationships into feature attribution while preserving many desirable properties of SHAP. By combining the *Peter-Clark* (PC) algorithm for causal discovery and the *Intervention Calculus when the DAG is Absent* (IDA) algorithm for causal strength quantification, our approach addresses the weakness of SHAP. Specifically, Causal SHAP reduces attribution scores for features that are merely correlated with the target, as validated through experiments on both synthetic and real-world datasets. This study contributes to the field of Explainable AI (XAI) by providing a practical framework for causal-aware model explanations. Our approach is particularly valuable in domains such as healthcare, where understanding true causal relationships is critical for informed decision-making.

## I. INTRODUCTION

As machine learning models become more sophisticated, their complexity creates a black-box conundrum [1], where the lack of transparency undermines trust. As models are deployed in high-stakes decision-making tasks, such as autonomous driving and medical diagnosis, and face new regulatory requirements like the EU AI Act, the need for interpretable AI has become essential—not only for legal compliance but also for ensuring alignment with societal standards.

One of the most widely used machine learning interpretability methods is SHapley Additive exPlanations (SHAP) [2]. SHAP is inspired by Shapley values [3], a game theory concept that quantifies each player’s contribution in a cooperative setting. A key limitation of SHAP and its common variations is their inability to capture a fundamental aspect of real-world systems: causality [5]. While SHAP makes the correlations learned by predictive ML models transparent, it disregards causal relationships among model inputs. This limitation arises from its assumption of feature independence, which can lead to misattributed feature importance [12] and the generation of impossible feature combinations [26].

For example, in Figure 1, SHAP (left) assigns importance based on correlations, suggesting that all features have direct edges to lung cancer, implying that they all directly contribute to the “lung cancer” prediction. However, domain knowledge (right) reveals that not all features have a direct path to lung

cancer and that some features are dependent on others. As a result, SHAP misattributes importance and fails to account for causal relationships between features. This limitation is particularly problematic in healthcare, where incorrect feature attribution could lead to misguided therapeutic decisions.

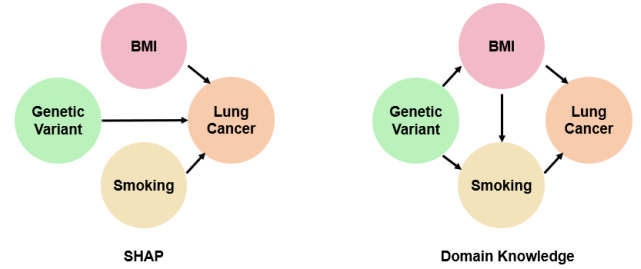


Fig. 1. On the left, we see the standard SHAP calculation of feature attribution. All three cancer risk factors, BMI, Genetic Variant, and Smoking are considered equally. However, studies have shown that Smoking and BMI both act as mediators in the causal graph [25]. Thus, to correctly quantify their importance, we must account for these causal relationships in feature attribution.

Recent approaches have attempted to address this limitation by integrating causality into SHAP, including On-Manifold Shapley Values [19], Asymmetric Shapley Values (ASV) [5], Causal Shapley Values [8], and Shapley Flow [10]. However, these methods still face challenges in efficiently handling feature dependencies and causality. They either require a complete causal graph for the algorithms to function or suffer from exponentially increasing computational complexity as the number of features grows.

In this paper, we propose a novel Causal SHAP framework that explains how each feature in the dataset contributes to the model’s prediction while respecting the causal relationships within the data. Specifically, our approach integrates causal relationships into SHAP calculations by employing the Peter-Clark (PC) algorithm [6] for causal edge discovery and the Intervention Calculus when the DAG is Absent (IDA) algorithm [7] for causal strength quantification. The PC algorithm is a constraint-based method that uses statistical tests to uncover causal relationships in data [6]. IDA builds upon the directed acyclic graphs (DAGs) inferred by PC to estimate causal effects using intervention calculus [7]. This combination allows us to model how features influence one another through directed causal paths, rather than treating all

correlations equally. Both PC and IDA are well-established and widely used techniques in causal discovery.

To validate the effectiveness of our approach, we evaluated Causal SHAP on both synthetic data with known causal structures and real-world datasets. We demonstrate that our method not only provides more accurate feature attributions but also better reflects the causal structure of the underlying datasets. Extensive experiments were conducted to highlight the advantages of our method.

In summary, the contributions of this paper are as follows:

- 1) A novel framework for integrating causality into SHAP using the PC algorithm for causal discovery between features and the IDA algorithm for quantifying causal strength.
- 2) Theoretical results showing that the proposed approach preserves the three key desired properties of SHAP: local accuracy, missingness, and consistency.
- 3) Experimental validation of Causal SHAP’s effectiveness through the insertion test and the RMSE between the computed SHAP scores and the ground truth.

## II. RELATED WORK

Recent work has attempted to integrate causality into SHAP through methods such as On Manifold Shapley Values [19], Asymmetric Shapley Values (ASV) [5], Causal Shapley values [8] and Shapley Flow [10]. On Manifold Shapley Values focuses on local explanation and attempts to provide more accurate explanations when features are dependent on each other. It does this by modifying the Shapley value function to condition out-of-coalition features on in-coalition features. However, the computational time scales exponentially as the number of features increases. Causal Shapley Values [8] proposed a node-based approach that incorporates Pearl’s do calculus to split attribution between parents and children in the a priori causal graph, allowing the method to capture both direct and indirect effects, but requires the complete causal graph to implement. When only partial causal information is available, Asymmetric Shapley Values (ASV) [5] provided a theoretical framework that relaxes the Axiom of Symmetry to allow non-uniform weighting of feature importance to integrate causality into model explainability, therefore providing a more nuanced explanation that can prioritise causal ancestor and descendant. Shapley Flow [10] further advanced this by assigning attribution to edges instead of nodes, and unified Shapley value based methods including ASV.

While these methods address the causal aspect, another key challenge is handling feature dependencies in practice. Popular implementations of SHAP variants (KernelSHAP [2], Interventional TreeSHAP [13], DeepSHAP [2]) assume feature independence for computational efficiency. Although TreeSHAP offers a path-dependent variant that can handle dependencies, it is limited to tree-based models and produces biased estimates [14]. To address feature dependencies, several approximation methods have been proposed, including approaches using multivariate Gaussian distributions with Kernel Estimation [11], as well as methods based on Gaussian

distributions, Gaussian copula distributions, or empirical distributions [12] to estimate conditional expectations.

However, as these frameworks are built on Shapley Values, they face exponential complexity as the number of features increases [4]. Hence, various approximation techniques have been proposed, including sampling-based approaches and model-specific optimizations [2]. Despite all these techniques, the efficient handling of both causality and feature dependencies remains an open challenge.

Existing causal attribution methods like ASV, Causal Shapley Values, and Shapley Flow typically assume access to a causal graph from domain experts, while recent advances in causal discovery offer promising alternatives for automatically inferring these relationships. However, these methods have not been integrated with SHAP frameworks.

## III. BACKGROUND

In this section, we briefly review key concepts used in this work, namely, Shapley values from cooperative game theory, SHAP for model explanations, Peter-Clark (PC) algorithm for causal discovery, and a causal effect estimation method named “Intervention calculus when the DAG is absent” (IDA).

a) *Shapley Values*: In cooperative game theory, the Shapley value of a player  $i$  represents their contribution to the payout and is computed as the weighted sum over all possible feature value combinations:

$$\phi_i = \sum_{S \subseteq N \setminus \{i\}} \frac{|S|!(n - |S| - 1)!}{n!} [v(S \cup \{i\}) - v(S)]. \quad (1)$$

Here,  $\phi_i$  represents the contribution of player  $i$  to the prediction;  $N$  is the set of all players;  $n$  is the number of players;  $S$  is a subset of players excluding player  $i$ ;  $v(S)$  is the value function defined as

$$v(S) = E[f(X)|X_S = x_S], \quad (2)$$

where  $f$  is the predictive model;  $X$  is the vector of input features (players); and  $X_S = x_S$  means we are conditioning on knowing the value in the subset of players  $S$  for this expectation calculation.

b) *SHAP*: SHAP is a method used to explain how each feature contributes to a prediction in a prediction model, using Shapley values. Although SHAP is model-agnostic, it makes the assumption of feature independence [12], which is rare in real-world data sets. The SHAP documentation states that the interventional expectation

$$v(S) = E[f(X)|do(X_S = x_S)] \quad (3)$$

is used to approximate the conditional expectation given in Eqn. 2, while computing SHAP values. The do-operator,  $do(X_S)$ , introduced by Pearl [22], represents an intervention that sets variables  $X_S$  to specific values  $x_S$  while ignoring any possible influence of the set of players  $N \setminus S$  on the set of interventions. This approximation is used for computational efficiency, as computing the true conditional expectation would require estimating complex conditional distributions and would scale exponentially with the number of features.

c) *Peter-Clark (PC)*: PC is a widely used constraint-based causal discovery algorithm [6] that constructs a causal graph in two phases: (1) initialization of the graph skeleton and (2) identification of the edge orientation, as illustrated in Figure 2.

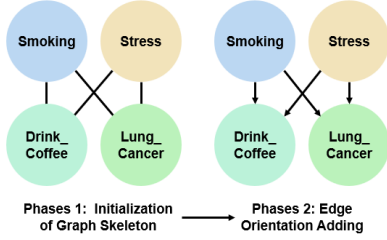


Fig. 2. An example of two phases in PC algorithm

Starting with a fully connected undirected graph (assuming full interactions between all features), phase 1 systematically removes edges between conditionally independent pairs based on statistical tests, i.e., for each pair of variables found to be conditionally independent given a set of other variables (called the separating set), the edge between the pair is removed. These tests are performed with increasingly large conditioning sets. The output of the first phase is a graph skeleton that shows causal relationships between pairs of variables. In the second phase, PC first identifies v-colliders [6] where non-adjacent variables share a common neighbor not in their separating set, then applies orientation rules to form a completed partially directed acyclic graph (CPDAG).

d) *IDA*: Using the CPDAG computed with PC, IDA finds the parents of each variable and estimates the causal effects between all pairs of parents and children. As multiple DAGs can be extracted from a CPDAG, IDA uses Pearl’s do-calculus to obtain a multi-set of possible causal effects, as illustrated in Fig. 3. For each DAG, IDA estimates non-negative edge weights representing causal strength using regression for all edges [18].

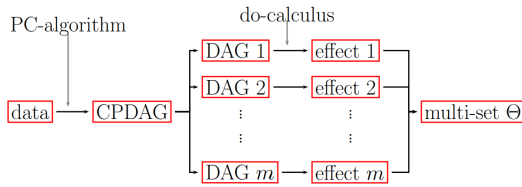


Fig. 3. An illustration of IDA (adapted from [7]).

## IV. METHODOLOGY

### A. Problem Setting

To infuse causality into SHAP, we introduce Causal SHAP to attribute a model prediction to its input features, while respecting known causal relationships between variables.

Considering the following *feature attribution* problem: Given a prediction model  $f : \mathcal{X} \rightarrow \mathbb{R}$  where  $\mathcal{X} \subseteq \mathbb{R}^n$  and an instance  $x = (x_1, \dots, x_n) \in \mathcal{X}$ , derive the contribution of each feature to the models prediction  $f(x)$  (Definition IV.1).

**Definition IV.1** (Feature Attribution). Given an instance  $x$ , a *feature attribution method*  $\zeta$  is a mapping  $\zeta(x; f) : \mathcal{X} \rightarrow \mathbb{R}^n$ , with each  $\phi_i = \zeta(x; f)_i$  quantifying the contribution of the feature  $i$  to  $f(x)$ .

In this work, we model the causal relationships between variables using a DAG,  $G = (V, E)$  where:  $V = \{1, \dots, n\}$  is the set of features and  $E \subseteq V \times V$  represents causal relationships between features. For each feature  $i \in V$ ,  $PA_i = \{j : (j, i) \in E\}$  denotes its parent set and  $W_i$  its total causal effect on the prediction target  $Y$ . Note that  $W_i$  is computed using causal effects between edges found with the IDA algorithm.

Our objective is to compute feature attributions  $\{\phi_i\}_{i=1}^n$  that follow the SHAP approach, while satisfying the key properties: local accuracy, missingness and consistency (see Section V for their definitions) and reflect both:

- Direct effects: Causal strength through edges  $(i, Y)$ .
- Indirect effects: Causal strength through paths  $i \rightsquigarrow Y$ .

The key challenge lies in effectively computing these attributions while accounting for the causal structure in  $G$ .

### B. Method

We propose a two-step modification to SHAP to account for causality in its feature attribution as illustrated in Figure 4. Firstly, we introduce a new value function (*Causal Value Function*) to better approximate the Shapley value function (Equation 2) than SHAP’s interventional expectation (Equation 3) by preventing the generation of impossible data points in its sampling-based calculation. Next, we consider causal strength integration to assign different strengths to different causal edges, effectively discounting feature attribution values with “causal strength”.

The causal value function is inspired by causal intervention, in which one observes changes in the output while manipulating the input. In our context, we incorporate Pearl’s do-operator, which isolates the causal effect of a subset of variables by fixing their values, and sampling the other variables outside of the subset, with respect to the causal graph. The difference between our method (Eqn 4) from the original SHAP (Eqn 3) is that we sample the out-of-coalition features with respect to the causal relationship, hence prevent the generation of impossible data points that would not happen in real-life. The causal relationship is based on the causal graph computed using the PC algorithm:

$$v_c(S) = \mathbb{E} \left[ f(X) \mid \text{do}(X_S = x_S), \right. \\ \left. X_{\bar{S}} \sim \text{Pr}(X_{\bar{S}} \mid \text{do}(X_S = x_S)) \right]. \quad (4)$$

Here,  $\text{do}(X_S = x_S)$  represents Pearl’s do-operator.  $\bar{S} = \{i \in 1, \dots, n \mid i \notin S\}$  denotes the set of variables not in  $S$ .  $\text{Pr}(X_{\bar{S}} \mid \text{do}(X_S = x_S))$  represents the distribution of variables not in  $S$ , given the intervention on variables in  $S$ .

The distribution  $\text{Pr}(X_{\bar{S}} \mid \text{do}(X_S = x_S))$  is determined by the causal mechanisms, specifically, it depends on whether these variables have parents in the causal graph. For a variable

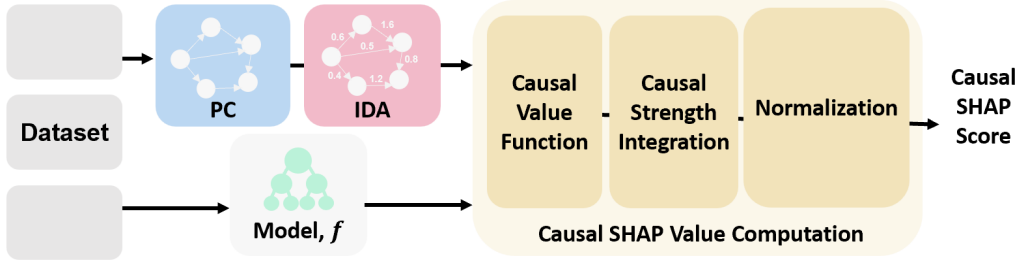


Fig. 4. Causal SHAP Framework: A pipeline for integrating causality into SHAP feature attribution. The framework consists of three main components: (1) PC algorithm for discovering causal relationship between features. (2) IDA algorithm for estimating the strength of causal effect. (3) Causal SHAP value computation to incorporate both causal structure and strength information through Causal Value Function, Causal Strength Integration and followed by a normalization step to maintain additivity. This approach combines causal discovery with feature attribution while preserving SHAP’s desirable properties.

$X_i \in X_{\bar{S}}$  that has no parents in the causal graph, its distribution remains unchanged:

$$X_i \sim \Pr(X_i), \quad (5)$$

where  $\Pr(X_i)$  is the original marginal distribution of  $X_i$ . For a variable  $X_i \in X_{\bar{S}}$  that has parents  $\text{PA}_i$  in the causal graph, its distribution is conditioned on the values of its parents:

$$X_i \sim N(\mu_i, \sigma_i), \quad (6)$$

where  $\mu_i$  is estimated using linear regression of  $X_i$  based on its parents  $\text{PA}_i$ , and  $\sigma_i$  is estimated from the regression residuals. When computing the causal value function  $v_c(S)$ , we sample the values of variables in  $X_{\bar{S}}$  from their respective distributions, as described above. This ensures that the values of variables not in  $S$  are consistent with the causal relationships in the graph, given the interventions performed on variables in  $S$ .

The total causal effect  $W_i$  for each feature  $i$  on target  $Y$  is computed by analyzing all possible paths in the IDA multi-set output from feature  $i$  to  $Y$ . For a given path  $p$ , the path-specific effect  $W_i^p$  on target  $Y$  is calculated as the product of individual edge weights (mean causal effects) along that path:

$$W_i^p = \prod_{(j,k) \in p} w_{jk}, \quad (7)$$

where  $w_{jk}$  represents the edge weight between nodes  $j$  and  $k$  retrieved from IDA algorithm. The total causal effect  $W_i$  for feature  $i$  is then computed as the sum of effects across all paths:

$$W_i = \sum_{p \in P_i} W_i^p, \quad (8)$$

where  $P_i$  is the set of all simple paths from feature  $i$  to the target  $Y$ .<sup>1</sup> Then, we integrate causal strength into SHAP to ensure that it accounts for information from the causal graph. The causal weight factor  $\gamma_i$  is defined as:

$$\gamma_i = \frac{|W_i|}{\sum_{j \in N} |W_j|}, \quad (9)$$

<sup>1</sup>While PC produces a CPDAG,  $P_i$  represents directed paths in DAGs from the IDA equivalence class, which are finite due to acyclicity of the graph.

where  $W_i$  represents the total causal effect of feature  $i$  on the target variable, computed using the IDA algorithm [7]. Hence, our novel *Causal SHAP* value is defined as:

$$\phi_i^c = \sum_{S \subseteq N \setminus \{i\}} w(S, i) [v_c(S \cup \{i\}) - v_c(S)], \quad (10)$$

where

$$w(S, i) = \frac{|S|!(n - |S| - 1)!}{n!} \gamma_i.$$

Lastly, we normalize the causal SHAP values with:

$$\phi_i^n = \phi_i^c \times \frac{f(x) - E[f(X)]}{\sum_{j=1}^n \phi_j^c}. \quad (11)$$

## V. THEORETICAL EVALUATION

SHAP is known for its good properties: local accuracy, missingness, and consistency. Together, they imply the four Shapley value axioms [2].

- **Local Accuracy:** The explanation for an instance should reflect the prediction probability for that instance as given by the predictor.
- **Missingness:** Any instance missing a feature-value should assign a zero attribution value to that missing feature.
- **Consistency:** For any two prediction models where one has a larger change in prediction with the removal of a feature than another. Then the resulting explanation for that feature should be larger.

We show that the proposed normalised Causal SHAP maintain these properties as follows, starting with the Local Accuracy

**Theorem V.1 (Local Accuracy).** *For any model  $f$  and features  $X$ , the normalized causal SHAP values satisfy:*

$$\sum_{i \in N} \phi_i^n = f(x) - \mathbb{E}[f(X)], \quad (12)$$

where  $N$  is the set of all features in the causal graph.

*Proof.* By construction, our normalization step ensures:

$$\begin{aligned} \sum_{i \in N} \phi_i^n &= \sum_{i \in N} \phi_i^c \times \frac{f(x) - \mathbb{E}[f(X)]}{\sum_{j=1}^n \phi_j^c} \\ &= (f(x) - \mathbb{E}[f(X)]) \times \frac{\sum_{i \in N} \phi_i^c}{\sum_{j=1}^n \phi_j^c} \\ &= f(x) - \mathbb{E}[f(X)]. \end{aligned}$$

□

**Theorem V.2** (Missingness). *Let  $G = (V, E)$  be the causal graph and  $i$  be a feature. If  $i \notin V$  or  $i$  has no path to the target variable in  $G$ , then  $\phi_i^c = 0$ .*

*Proof.* This follows from two cases. Firstly, if  $i \notin V$ , then by definition  $W_i = 0$  and thus  $\gamma_i = \frac{|W_i|}{\sum_{j \in N} |W_j|} = 0$ . Secondly, if  $i$  has no path to the target, then  $|W_i| = 0$  as there is no causal effect, again leading to  $\gamma_i = 0$ . In both cases,  $\phi_i^c = 0$ . □

**Theorem V.3** (Consistency). *Let  $f_x(z') = f(h_x(z'))$ , where  $h_x$  maps simplified inputs to original inputs, and let  $z' \setminus i$  denote setting  $z'_i = 0$ . For any two models  $f$  and  $f'$ , if:*

$$f'_x(z') - f'_x(z' \setminus i) \geq f_x(z') - f_x(z' \setminus i) \quad (13)$$

*holds for all  $z' \in \{0, 1\}^M$ , then:*

$$\phi_i^c(f', x) \geq \phi_i^c(f, x), \quad (14)$$

*where  $\phi_i^c(\cdot, x)$  denotes the Causal SHAP value for feature  $i$  at point  $x$ .*

*Proof.* From Eqn 10, we have

$$\phi_i^c(f, x) = \sum_{S \subseteq N \setminus \{i\}} w(S, i) [f_x(S \cup \{i\}) - f_x(S)],$$

where  $w(S, i) = \frac{|S|!(M-|S|-1)!}{M!} \gamma_i$  and  $\gamma_i = \frac{|W_i|}{\sum_{j \in N} |W_j|}$  is determined by the total causal effect  $W_i$  on the target. Let  $\Delta f_x(S) = f_x(S \cup \{i\}) - f_x(S)$  denote the marginal contribution of feature  $i$  given subset  $S$ . Since  $f$  and  $f'$  share the same causal structure,  $\gamma_i$  remains constant. Then:

$$\begin{aligned} & \phi_i^c(f', x) - \phi_i^c(f, x) \\ &= \sum_{S \subseteq N \setminus \{i\}} w(S, i) [\Delta f'_x(S) - \Delta f_x(S)] \\ &= \sum_{S \subseteq N \setminus \{i\}} w(S, i) [\Delta f'_x - \Delta f_x] \\ &\geq 0. \end{aligned}$$

The final inequality follows from:  $w(S, i) \geq 0$  for all  $S$  since both the Shapley kernel and  $\gamma_i$  are non-negative,  $\Delta f'_x \geq \Delta f_x$  by the hypothesis of the theorem, the causal structure (and thus  $\gamma_{i,s}$ ) remains unchanged between  $f$  and  $f'$ . Therefore,  $\phi_i^c(f', x) \geq \phi_i^c(f, x)$ . □

Note that although Theorems V.2 and V.3 are shown with respect to  $\phi_i^c$ , it is easy to see that they hold for  $\phi_i^n$  as well.

## VI. ALGORITHM AND EXPERIMENTS

We provide a detailed algorithm for computing Causal SHAP as shown in Algorithm 1. As computing Shapley value is expensive, sampling methods are widely used. In our work, Monte Carlo sampling is used to approximate  $v_c$  as follows:

$$v_c(S) \approx \frac{1}{M} \sum_{m=1}^M f(x_S, \tilde{x}_S^{(m)}), \quad (15)$$

---

### Algorithm 1 Causal SHAP Value Computation.

---

**Require:**

- 1:  $f : \mathcal{X} \rightarrow \mathbb{R}$  : trained model
- 2:  $x \in \mathcal{X}$  : instance to explain
- 3:  $G = (V, E)$  : causal graph from PC algorithm
- 4:  $\{W_i\}_{i=1}^n$  : total causal effects from IDA algorithm
- 5:  $T$  : number of Monte Carlo samples

**Ensure:** Normalized causal Shapley values  $\{\phi_i^n\}_{i=1}^n$

- 6: Compute causal weight factors:  $\gamma_i \leftarrow \frac{|W_i|}{\sum_{j=1}^n |W_j|}$  for  $i \in \{1, \dots, n\}$
  - 7: Initialize:  $\phi_i^c \leftarrow 0$  for  $i \in \{1, \dots, n\}$
  - 8:  $\mathbb{E}[f(X)] \leftarrow \frac{1}{m} \sum_{j=1}^m f(x_j)$  where  $\{x_j\}_{j=1}^m$  is training data
  - 9: **for**  $t = 1$  to  $T$  **do**
  - 10:  $S \leftarrow$  uniform random subset of  $\{1, \dots, n\}$
  - 11: **for**  $i \in \{1, \dots, n\} \setminus S$  **do**
  - 12:  $v_c(S)$  via Monte Carlo sampling on  $G$
  - 13:  $v_c(S \cup \{i\})$  via Monte Carlo sampling on  $G$
  - 14:  $w \leftarrow \frac{|S|!(n-|S|-1)!}{n!} \times \gamma_i$
  - 15:  $\phi_i^c \leftarrow \phi_i^c + w(v_c(S \cup \{i\}) - v_c(S))$
  - 16: **end for**
  - 17: **end for**
  - 18: Normalize:  $\phi_i^n \leftarrow \phi_i^c \times \frac{f(x) - \mathbb{E}[f(X)]}{\sum_{j=1}^n \phi_j^c}$  for  $i \in \{1, \dots, n\}$
  - 19: **return**  $\{\phi_i^n\}_{i=1}^n$
- 

where  $M$  is the number of Monte Carlo samples,  $\tilde{x}_S^{(m)}$  is the  $m$ -th sample of non-intervened features. Samples are generated through the following process. For each feature  $i \in \bar{S}$ , in topological order:

- If feature has no parents: sample from its marginal distribution
- Otherwise: sample from  $\mathcal{N}(\mu_i, \sigma_i)$  where:  $\mu_i$  is the predicted mean from linear regression conditioned on parent values and  $\sigma_i$  is estimated from regression residuals

In addition to using Monte Carlo, we use multiprocessing pool to parallelize the Causal SHAP computation on AMD EPYC 7713 in our experiments.

We evaluated our approach with four datasets (see Table I). With the two synthetic datasets (one with only direct causal effects and another one with both direct and indirect causal effects), we assess how well each method captures true causal relationships, using the known causal graph as a reference (as the datasets are synthetic with known graph ground truth). Secondly, SHAP is also applied to a reduced feature set (a subset of the features that have a direct causal path to the target variable, without being influenced by other features) and served as a ground truth to evaluate how well each method captures the true causal effect. For the two real-world datasets, we use the *insertion score* [15], which is a standard metric used for feature attribution evaluation in e.g. [23] and [24] to evaluate the performance.

For benchmarking, we compare our Causal SHAP method with 5 other SHAP-derived methods: Independent SHAP [2], Kernel SHAP [2], On Manifold SHAP [19], Shapley Flow [10]



and Asymmetric Shapley Values (ASV) [5]. Note that other feature-attribution methods such as LIME [9] are omitted due to our focus on SHAP-derived methods.

#### 1) Synthetic Datasets:

a) *Lung Cancer*: Features in this dataset are *smoking*, *stress*, and *drink\_coffee*, with *lung\_cancer\_risk* as the target variable. The *stress* and *smoking* are both generated using a normal distribution  $\mathcal{N}(5, 2)$ . The relationships between the variables are inspired by cancer research [25], [27], [28] and are defined as:

$$\text{lung\_cancer\_risk} = 2 \cdot \text{smoking} + 1.2 \cdot \text{stress} + \epsilon_{\text{risk}}, \quad (16)$$

$$\text{drink\_coffee} = 2 \cdot \text{smoking} + \text{stress} + \epsilon_{\text{coffee}}, \quad (17)$$

where  $\epsilon_{\text{risk}} \sim \mathcal{N}(0, 3)$  and  $\epsilon_{\text{coffee}} \sim \mathcal{N}(0, 1)$  represent independent noise terms sampled from normal distributions. The parameters in Equations 16 and 17 are chosen to generate synthetic data that exhibits clear causal relationships, allowing us to validate our causal discovery method by comparing the PC algorithm's output against a known ground truth causal structure. The causal graph successfully recovered by the PC algorithm from this data set is shown in Figure 5.

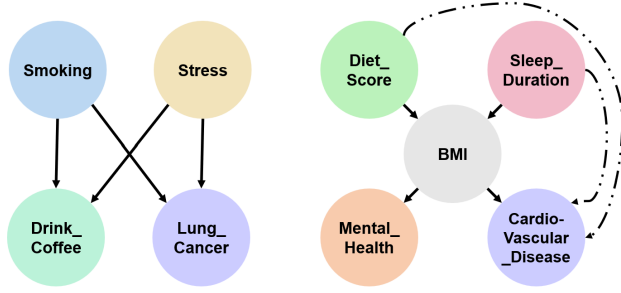


Fig. 5. Diagram shows the causal graph of Lung Cancer Data set (Left), and the causal graph of Cardiovascular disease (Right). Solid arrow indicates causal edge with direct effect generated from PC algorithm, dashed lines represent the indirect effect.

In the graph, *smoking* and *stress* act as confounders, influencing and creating a non-causal correlation between *lung\_cancer\_risk* and *drink\_coffee*. With this design, we expect a causally-aware attribution method to assign significant SHAP values to *smoking* and *stress*, as they are direct causes, while assigning near-zero SHAP value to *drink\_coffee*, despite its correlation with *lung\_cancer\_risk*. This allows us to differentiate between methods that only capture statistical associations versus those that successfully incorporate causal relationships.

In Figure 5, we observe that Causal SHAP attributes a zero SHAP score to *drink\_coffee* in accordance with the causal graph. While Kernel SHAP misattributes significant scores to *drink\_coffee*, and fails to distinguish between causality and correlation.

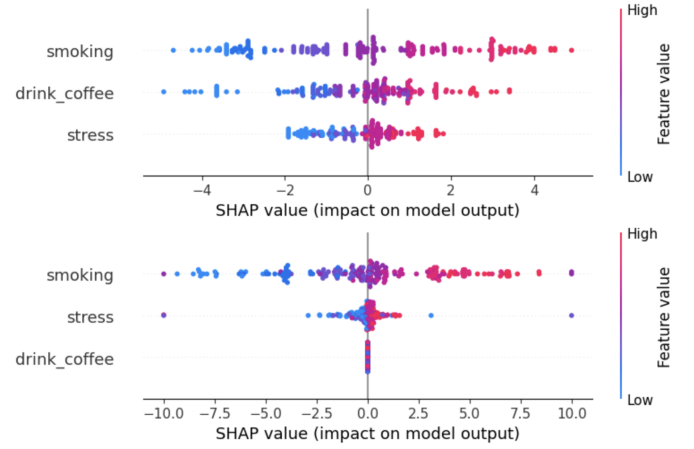


Fig. 6. Kernel SHAP (top) versus Causal SHAP (bottom) for features in Lung Cancer Synthetic Dataset, *drink\_coffee* in Causal SHAP is correctly attributed zero score as it is not affecting *Lung\_Cancer\_Risk*

Of all the methods listed in Table II, Causal SHAP achieved the lowest Root Mean Squared Error (RMSE) against ground truth, best capturing the true causal effects. Independent SHAP, Kernel SHAP, and On Manifold SHAP failed to capture causality. Shapley Flow and ASV successfully give a near-zero score to *drink\_coffee*, but unfortunately have a larger discrepancy in score on other variables.

b) *Cardiovascular Diseases*: This dataset has *diet\_score*, *sleep\_duration*, and *family\_history* as input. The first is randomly generated from a uniform distribution  $\mathcal{U}(1, 10)$ , while the latter two come from  $\mathcal{N}(8, 4)$  and  $\mathcal{N}(4, 2)$  distributions.

$$\text{bmi} = 0.4 \cdot \text{diet\_score} + 0.5 \cdot \text{sleep\_duration} + \epsilon_{\text{bmi}}, \quad (18)$$

$$\text{mental\_health} = 1.5 \cdot \text{bmi} + \epsilon_{\text{health}}, \quad (19)$$

$$\text{cv\_risk} = 1.5 \cdot \text{bmi} + \epsilon_{\text{risk}}, \quad (20)$$

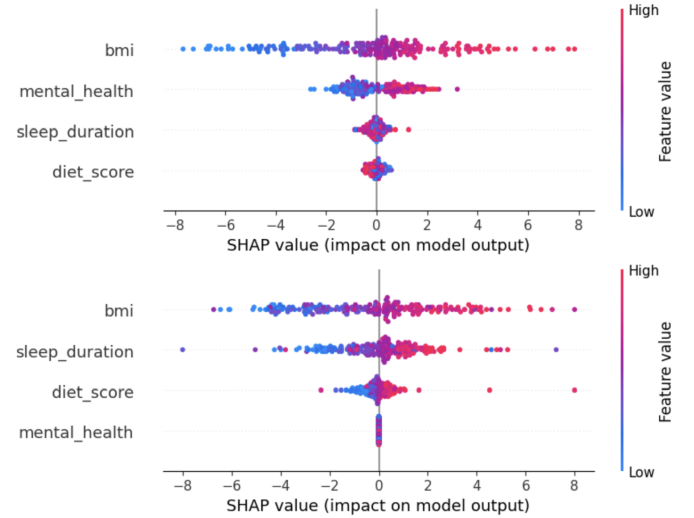


Fig. 7. Kernel SHAP (top) versus Causal SHAP (bottom) for features in Cardiovascular Disease Synthetic Dataset, *mental\_health* is correctly attributed zero score while *diet\_score* and *sleep\_duration* are assigned higher scores due to their indirect effect to *CV\_risk*.

TABLE I  
SUMMARY OF DATASETS.

Dataset	# Features	Train Size	Test Size	Problem	Data Type
Lung Cancer Risk	4	800	200	Regression	Synthetic
Cardiovascular Risk	5	800	200	Regression	Synthetic
Irritable bowel syndrome (IBS)	31	294	74	Classification	Real-world
Colorectal Cancer	21	18321	4580	Classification	Real-world

TABLE II  
COMPARISON OF SHAP METHODS ON SYNTHETIC DATASET 1 & 2. **BOLD** VALUES INDICATE THE BEST PERFORMANCE AND UNDERLINE VALUES INDICATE SECOND BEST.

Feature (Lung Cancer)	Ground Truth	Causal SHAP	Independent SHAP	Kernel SHAP	On Manifold	Shapley Flow	ASV
Smoking	5.2171	5.3462	3.9467	3.2405	2.0104	2.1600	5.9366
Stress	0.2507	0.2600	0.1031	0.3620	1.8759	0.2600	1.9125
Drink Coffee	–	0.0000	1.8163	1.9514	1.9798	0.0000	-0.0805
<b>RMSE</b>	–	<b>0.0167</b>	<u>1.6357</u>	3.9193	12.9241	8.8037	3.2792

Feature (Cardiovascular Risk)	Ground Truth	Causal SHAP	Independent SHAP	Kernel SHAP	On Manifold	Shapley Flow	ASV
Diet Score	0.5526	0.2397	-0.5545	-0.1910	1.3073	2.4000	0.0288
Sleep Duration	3.6362	2.2416	0.1123	0.3247	1.1862	3.9300	0.0401
BMI	–	3.6056	4.1359	4.2996	1.3811	3.0900	4.9054
Mental Health	–	0.0000	1.3065	1.7032	1.3838	0.0000	0.2841
<b>RMSE</b>	–	<b>2.0422</b>	13.6421	11.5176	6.5710	<u>3.4993</u>	13.2048

where  $\epsilon_{bmi} \sim \mathcal{N}(0, 1)$ ,  $\epsilon_{health} \sim \mathcal{N}(0, 1)$  and  $\epsilon_{risk} \sim \mathcal{N}(2, 3)$  are independent noise added to the features. The parameters in Eqns 18-20 are inspired by [29] [30] [31] [32] and chosen to generate synthetic data with clear causal relationships. Figure 5 shows the causal graph recovered by the PC algorithm.

Similar to the previous dataset, we have *bmi* that acts as our confounder. We expect a causally-aware attribution method to assign significant SHAP values to *bmi* as it is the direct cause, at the same time assign a lower but non-zero SHAP values to *diet\_score* and *sleep\_duration* as they are the indirect causes.

In Figure 7, Causal SHAP successfully attributes zero score to *mental\_health* and also provides a higher importance to *sleep\_duration* and *diet\_score* because these are the two factors that causally affect *bmi*. While Kernel SHAP failed to distinguish correlation and causation, it did not manage to capture the causal links of *sleep\_duration* nor *diet\_score* thus assigned near zero scores to them.

Referring to Table 2, Causal SHAP achieved the lowest RMSE compared to Ground Truth, best capturing the true causal effects of *diet\_score* and *sleep\_duration*. Note that *mental\_health* is omitted as it lacks a path to *CV\_risk*, and *bmi* is excluded because its causal relationship with two other variables, which may make it difficult to interpret the Ground Truth values for BMI in terms of the true causal effects.

2) *Real-World Datasets*: We evaluated our method on two biomedical datasets: IBS [20] and Colorectal cancer datasets [21], selected for their high complexity of causal links between metabolites, lifestyle factors, physiological measurements, and genetic information. We compared Causal SHAP against five baseline methods using the insertion test [15], which sequentially adds features from most to least important based on each method’s attributions, measuring AUROC, Cross Entropy and Brier scores at each step. High AUROC, lower Cross Entropy and Brier scores indicate better performance. All experiments

used the same Random Forest model as the black box.

As shown in Table III, Causal SHAP achieved:

- On IBS dataset: Best AUROC (0.8594) and second-best Cross Entropy (0.4645) and Brier scores (0.1464)
- On Colorectal Cancer dataset: Best performance across all metrics (AUROC: 0.6271, Cross Entropy: 0.6735, Brier: 0.2397)

While Shapley Flow and ASV incorporate causal information via PC and IDA algorithms, Causal SHAP’s superior performance suggests it leverages causal relationships more effectively. On Manifold performed strongly with IBS data, possibly because its dependency-agnostic approach works better when causal relationships are uncertain.

Computationally, we studied the impact of the hyperparameter  $M$  in Equation 15. We find that AUROC is not sensitive to changes in  $M$  once it exceeds 64. (e.g., IBS dataset:  $M=32$  yields AUROC=0.5678;  $M=64$  yields AUROC=0.5680). We also analyzed the computational cost of different components in our pipeline. To compute feature attributions for all IBS instances, the Causal SHAP Value Computation, PC, and IDA take 366.13, 0.26, and 1.56 seconds, respectively.

## VII. CONCLUSION AND FUTURE WORK

In this paper, we introduced Causal SHAP, a comprehensive feature attribution explainable AI method that considers causality between input features. Causal SHAP leverages the PC algorithm for causal path discovery and the IDA algorithm to estimate causal strength. Through experiments on multiple synthetic and real-world datasets, we demonstrated several key advantages of our method:

- 1) It effectively respects causal relationships, even in the presence of highly correlated features.
- 2) It achieves superior insertion scores on real-world datasets, even when the true causal graph is unknown.

TABLE III  
MAIN RESULTS: COMPARISON OF GLOBAL FEATURE ATTRIBUTION  
METHODS

	Insertion Score		
	AUROC	Cross Entropy	Brier
IBS			
- Independent SHAP	0.8527 $\pm$ 0.0326	0.4779 $\pm$ 0.0336	0.1517 $\pm$ 0.0136
- Kernel SHAP	0.8548 $\pm$ 0.0284	0.4674 $\pm$ 0.0360	0.1474 $\pm$ 0.0148
- On Manifold	<u>0.8589 <math>\pm</math> 0.0244</u>	<b>0.4644 <math>\pm</math> 0.0311</b>	<b>0.1461 <math>\pm</math> 0.0132</b>
- Shapley Flow	0.8274 $\pm$ 0.0359	0.5233 $\pm$ 0.0434	0.1706 $\pm$ 0.0178
- ASV	0.8225 $\pm$ 0.0356	0.5327 $\pm$ 0.0414	0.1756 $\pm$ 0.0174
- Causal SHAP	<b>0.8594 <math>\pm</math> 0.0227</b>	<u>0.4645 <math>\pm</math> 0.0314</u>	<u>0.1464 <math>\pm</math> 0.0134</u>
Colorectal Cancer			
- Independent SHAP	0.5886 $\pm$ 0.0337	0.6893 $\pm$ 0.0175	0.2475 $\pm$ 0.0080
- Kernel SHAP	<u>0.6263 <math>\pm</math> 0.0149</u>	0.6766 $\pm$ 0.0090	0.2410 $\pm$ 0.0040
- On Manifold	<u>0.6243 <math>\pm</math> 0.0132</u>	0.6781 $\pm$ 0.0081	0.2416 $\pm$ 0.0035
- Shapley Flow	0.5868 $\pm$ 0.0262	0.6864 $\pm$ 0.0148	0.2463 $\pm$ 0.0069
- ASV	0.6177 $\pm$ 0.0170	<u>0.6750 <math>\pm</math> 0.0087</u>	<u>0.2406 <math>\pm</math> 0.0039</u>
- Causal SHAP	<b>0.6271 <math>\pm</math> 0.0190</b>	<b>0.6735 <math>\pm</math> 0.0096</b>	<b>0.2397 <math>\pm</math> 0.0044</b>

<sup>1</sup> All results are averaged over 5 runs with different random seeds.  $\mu$  represents the mean and  $\sigma$  represents the standard deviation.

<sup>2</sup> Bold values indicate the best performance and underline values indicate second best for each dataset and metric.

### 3) It preserves key theoretical properties of SHAP.

We chose the PC algorithm due to its widespread use, under the assumption that no hidden variables influence the dataset. In future work, we aim to (1) address cases with hidden variables using the FCI algorithm [16] for causal graph estimation; (2) Explore Greedy Equivalence Search (GES) [17] when the PC algorithm becomes computationally expensive as number of features scale; (3) Enhance our framework to handle causal structure uncertainty in by aggregating multiple possible causal graphs. (4) Develop more efficient approximation algorithms for high-dimensional datasets with complex dependency structures.

### ACKNOWLEDGEMENT

This research is supported by the Ministry of Education, Singapore (Grant IDs: RG22/23, RS15/23, LKCMedicine Start up Grant).

### REFERENCES

- [1] Vilone, G. & Longo, L. Notions of explainability and evaluation approaches for explainable artificial intelligence. *Information Fusion*. **76** pp. 89-106 (2021)
- [2] Lundberg, S. A unified approach to interpreting model predictions. *ArXiv Preprint ArXiv:1705.07874*. (2017)
- [3] Shapley, L. A value for n-person games. *Contribution To The Theory Of Games*. **2** (1953)
- [4] Michalak, T., Aadithya, K., Szczepanski, P., Ravindran, B. & Jennings, N. Efficient computation of the Shapley value for game-theoretic network centrality. *Journal Of Artificial Intelligence Research*. **46** pp. 607-650 (2013)
- [5] Frye, C., Rowat, C. & Feige, I. Asymmetric shapley values: incorporating causal knowledge into model-agnostic explainability. *Advances In Neural Information Processing Systems*. **33** pp. 1229-1239 (2020)
- [6] Spirtes, P., Glymour, C. & Scheines, R. Causation, prediction, and search. (MIT press, 2001)
- [7] Maathuis, M., Colombo, D., Kalisch, M. & Bühlmann, P. Predicting causal effects in large-scale systems from observational data. *Nature Methods*. **7**, 247-248 (2010)

- [8] Heskies, T., Sijben, E., Bucur, I. & Claassen, T. Causal shapley values: Exploiting causal knowledge to explain individual predictions of complex models. *Advances In Neural Information Processing Systems*. **33** pp. 4778-4789 (2020)
- [9] Ribeiro, M., Singh, S. & Guestrin, C. "Why should i trust you?" Explaining the predictions of any classifier. *Proceedings Of The 22nd ACM SIGKDD International Conference On Knowledge Discovery And Data Mining*. pp. 1135-1144 (2016)
- [10] Wang, J., Wiens, J. & Lundberg, S. Shapley flow: A graph-based approach to interpreting model predictions. *International Conference On Artificial Intelligence And Statistics*. pp. 721-729 (2021)
- [11] Janzing, D., Minorics, L. & Blöbaum, P. Feature relevance quantification in explainable AI: A causal problem. *International Conference On Artificial Intelligence And Statistics*. pp. 2907-2916 (2020)
- [12] Aas, K., Jullum, M. & Løland, A. Explaining individual predictions when features are dependent: More accurate approximations to Shapley values. *Artificial Intelligence*. **298** pp. 103502 (2021)
- [13] Lundberg, S. & Others From local explanations to global understanding with explainable AI for trees. *Nature Machine Intelligence*. **2**, 56-67 (2020)
- [14] Amoukou, S., Salaün, T. & Brunel, N. Accurate shapley values for explaining tree-based models. *International Conference On Artificial Intelligence And Statistics*. pp. 2448-2465 (2022)
- [15] Petsiuk, V. Rise: Randomized Input Sampling for Explanation of black-box models. *ArXiv Preprint ArXiv:1806.07421*. (2018)
- [16] Richardson, T. A discovery algorithm for directed cyclic graphs. *ArXiv Preprint ArXiv:1302.3599*. (2013)
- [17] Meek, C. Graphical Models: Selecting causal and statistical models. (Carnegie Mellon University, 1997)
- [18] Kalisch, M., Mächler, M., Colombo, D., Maathuis, M. & Bühlmann, P. Causal inference using graphical models with the R package pcalg. *Journal Of Statistical Software*. **47** pp. 1-26 (2012)
- [19] Frye, C., Mijolla, D., Begley, T., Cowton, L., Stanley, M. & Feige, I. Shapley explainability on the data manifold. *ArXiv Preprint ArXiv:2006.01272*. (2020)
- [20] Jacobs, J. & Others Multi-omics profiles of the intestinal microbiome in irritable bowel syndrome and its bowel habit subtypes. *Microbiome*. **11**, 5 (2023)
- [21] Zhang, J. & Others APOE genotype modifies the association between midlife adherence to the planetary healthy diet and cognitive function in later life among Chinese adults in Singapore. *The Journal Of Nutrition*. **154**, 252-260 (2024)
- [22] Pearl, J. & Others Models, reasoning and inference. *Cambridge, UK: Cambridge University Press*. **19**, 3 (2000)
- [23] Covert, I., Lundberg, S. & Lee, S. Explaining by removing: A unified framework for model explanation. *Journal Of Machine Learning Research*. **22**, 1-90 (2021)
- [24] Wang, H. & Others Score-CAM: Score-weighted visual explanations for convolutional neural networks. *Proceedings Of The IEEE/CVF Conference On Computer Vision And Pattern Recognition Workshops*. pp. 24-25 (2020)
- [25] Zhou, W. & Others Causal relationships between body mass index, smoking and lung cancer: univariable and multivariable Mendelian randomization. *International Journal Of Cancer*. **148**, 1077-1086 (2021)
- [26] Hooker, G. & Mentch, L. Please stop permuting features: An explanation and alternatives. *ArXiv Preprint ArXiv:1905.03151*. **2** pp. 1 (2019)
- [27] Zhang, Y. & Others Psychological stress enhances tumor growth and diminishes radiation response in preclinical model of lung cancer. *Radiotherapy And Oncology*. **146** pp. 126-135 (2020)
- [28] Richards, G. & Smith, A. Caffeine consumption and self-assessed stress, anxiety, and depression in secondary school children. *Journal Of Psychopharmacology*. **29**, 1236-1247 (2015)
- [29] Wolongevicz, D. & Others Diet quality and obesity in women: the Framingham Nutrition Studies. *British Journal Of Nutrition*. **103**, 1223-1229 (2010)
- [30] Theorell-Haglöw, J. & Lindberg, E. Sleep duration and obesity in adults: what are the connections?. *Current Obesity Reports*. **5** pp. 333-343 (2016)
- [31] Luppino, F., Wit, L., Bouvy, P., Stijnen, T., Cuijpers, P., Penninx, B. & Zitman, F. Overweight, obesity, and depression: a systematic review and meta-analysis of longitudinal studies. *Archives Of General Psychiatry*. **67**, 220-229 (2010)
- [32] Ortega, F., Lavie, C. & Blair, S. Obesity and cardiovascular disease. *Circulation Research*. **118**, 1752-1770 (2016)